www.czasopisma.pan.pl PAN POLSKA AKADEMIA NAUK www.journals.pan.pl

DE GRUYTER OPEN

Arch. Min. Sci., Vol. 61 (2016), No 4, p. 853–873

Electronic version (in color) of this paper is available: http://mining.archives.pl

DOI 10.1515/amsc-2016-0057

GRZEGORZ KORTAS*

EQUILIZING OF THE PRIMARY STRESS STATE IN THE ROCK MASS, SIMULATED BY A MODEL OF LAYER IN AN ELASTIC-VISCOUS MEDIUM

WYRÓWNYWANIE NAPRĘŻEŃ PIERWOTNYCH W GÓROTWORZE SYMULOWANE MODELEM WARSTWY W OŚRODKU SPRĘŻYSTO-LEPKIM

This paper is devoted to the analysis of the stress development process in the homogeneous and non-homogeneous rock mass. The rock-mass model consists of an elastic-viscous medium containing a layer (Fig. 1) that displays distinct geomechanical strain properties. When examining the process of stress equilizing in time, the Norton-Bailey power creep law was applied in the numerical analysis. The relationship between effective stresses and time, the modulus of elasticity, Poisson's coefficient, and creep compliance were obtained. It was demonstrated that the relationship between effective stress and time or creep compliance, for the assumed conditions in a homogeneous rock-mass, was approximated by hyperbolic functions (10 and 16). The process parameter included a certain value of creep compliance or of time at which there occurred a half-way equilizing of primary stresses. An analogous function binds effective stresses with creep compliance. Our model studies indicated a number of relationships between bulk and shear strain with time and creep compliance in the homogeneous and non-homogeneous rock mass, presented in Figs. 2-14, expressed by the functions of those specific parameters.

The relationships obtained in this work resulted from our model assumptions. However, they demonstrated the influence of the geomechanical strain properties of rocks on the process of shaping the primary stress state in the rock mass and the tendency to reduce the principal stress differences in time. Our research results suggested the necessity to simulate the primary stress state as an initial condition of the geomechanical numerical analysis concerning the rock-mass behaviour showing rheological properties.

Keywords: primary stress state, non-homogeneous rock-mass, elastic-viscous medium, creep compliance, effective stress equilizing

Wielowiekowe procesy geodynamiczne, doprowadziły do wykształcania się obecnego stanu naprężeń w litosferze, który w zagadnieniach górniczych określa się pierwotnym stanem naprężeń górotworu. Praca poświęcona jest analizie długotrwałego procesu wykształcania się naprężeń w jednorodnym i niejednorodnym górotworze, przeprowadzonej w trybie badań modelowych. Określano zmiany naprężenia w ośrodku sprężysto-lepkiego z warstwą (Rys. 1), wykazującą odmienne odkształceniowe właściwości geomechaniczne. W obliczeniach numerycznych stosowano potęgowe prawo pełzania Nortona-Bailey'a.

* STRATA MECHANICS RESEARCH POLISH ACADEMY OF SCIENCES, UL. REYMONTA 27, 30-059 KRAKOW, POLAND

Kwantyfikatorem zmieniających się z upływem czasu różnic naprężeń głównych było średnie naprężenie efektywne w centralnym sektorze modelu geometrycznego badanego ośrodka. Otrzymano proste związki naprężeń efektywnych z czasem, modułem sprężystości, współczynnikiem Poissona i podatnością na pełzanie. Wykazano, że w jednorodnym górotworze związek naprężenia efektywnego z czasem lub z podatnością na pełzanie, aproksymuje funkcja hiperboliczna opisująca wyrównywanie naprężeń głównych (10 i 16). Wykazano, że parametrem procesu wyrównywania się naprężeń głównych jest pewna wartość podatności na pełzanie B_c lub czasu τ_c, przy których występuje połowiczne wyrównanie naprężeń początkowych. Wykazano, że w ośrodku sprężysto-lepkim z potęgowym prawem pełzania względny przyrost naprężeń jest odwrotnie proporcjonalny do czasu lub do podatności na pełzanie. Z badań modelowych wynika szereg związków odkształcalności objętościowej i postaciowej z czasem i podatnością dla jednorodnego i niejednorodnego górotworu, przedstawionych na rysunkach 2-14 i wyrażonych funkcjami tych parametrów.

Stwierdzono, że funkcja wyrównywania się naprężeń wyraża zasadę, że względny przyrost naprężeń jest odwrotnie proporcjonalny do zmiennej wymiarowej, którą może być czas lub podatność na pełzanie. W logarytmicznej skali czasu lub podatności wyodrębnić można trzy okresy lub przedziały. W drugim okresie (Rys. 2) i drugim przedziale zmian podatności (Rys. 6) następuje intensywne wyrównywanie się naprężeń efektywnych. Dla wartości średniej geometrycznej czasów na końcach tego przedziału τ_c lub podatności na pełzanie B_c naprężenie efektywne odpowiada połowie wartości naprężenia efektywnego na początku procesu. Stwierdzono, że wzrost wartości współczynnika Poissona nie wpływa na wartość τ_c, natomiast wzrost modułu Younga ośrodka powoduje spadek wartości τ_c. Wzrost podatności na pełzanie nie wpływa na początkowe naprężenia efektywne, ale powoduje wzrost τ_c i okresu wyrównywania się naprężeń. Stosunek τ_c dwóch ośrodków różniących się podatnością na pełzanie odpowiada stosunkowi ich podatności, a stosunek B_c dwóch procesów, w których zmienną jest podatność na pełzanie, odpowiada stosunkowi czasów ich trwania.

W ośrodku jednorodnym wykazującym właściwości reologiczne proces wyrównywania się naprężeń głównych prowadzi do utworzenia hydrostatycznego stanu naprężeń litostatycznych. Im podatność ośrodka na pełzanie jest większa, tym proces ten jest krótszy.

Stwierdzono, że w modelu niejednorodnego górotworu o odmiennych właściwościach warstwy i jej otoczenia proces wyrównywania się naprężeń jest tylko początkowo zgodny z funkcją hiperboliczną (11). Podobnie jak w ośrodku jednorodnym z upływem czasu naprężenia efektywne w warstwie dążą do zera. Początkowe naprężenie efektywne rośnie ze wzrostem modułu sprężystości warstwy oraz wydłużeniu ulega drugi okres wyrównywania naprężeń. Im wartość modułu sprężystości warstwy jest mniejsza, czyli im mniejsza jest różnica modułów sprężystości objętościowej warstwy i jej otoczenia, tym proces wyrównywania naprężeń jest dłuższy.

Różnicując podatność warstwy i jej otoczenia, funkcja wyrównywania się naprężeń w czasie rośnie i osiąga ekstremum, a czas, przy którym pojawia się to ekstremum zależy od stosunku podatności warstwy do podatności otoczenia. Zmiana podatności warstwy przy stałej podatności otoczenia prowadzi do równoległego przesunięcia w logarytmicznej skali czasu wykresu funkcji naprężeń efektywnych, przez co proces wyrównywania się naprężeń wydłuża się. Wartości naprężeń efektywnych z lokalnym ekstremum, występującym po krótkim okresie czasu, rosną prawie proporcjonalnie z głębokością. Po bardzo długim czasie wpływ głębokości zanika. Podobnie jak dla jednorodnego górotworu proces wyrównywania się naprężeń można przedstawić dla zmiennej podatności warstwy i czasu jako parametru przy zachowaniu stałej podatności otoczenia.

Wyniki badań przedstawione w tej pracy pokazują istotną rolę czasu i właściwości odkształceniowych skał w procesie kształtowania się naprężeń w ośrodku wykazującym właściwości reologiczne. Wskazują także, że w obliczeniach numerycznych stanu naprężeń wokół wyrobisk w ośrodkach niejednorodnych, naprężeniowe warunki początkowe w obszarach różniących się podatnością na pełzanie są odmienne. Taki stan naprężeń pierwotnych może być symulowany przez proces odwzorowujący długotrwałe oddziaływanie sił masowych.

Słowa kluczowe: naprężenia pierwotne, niejednorodność górotworu, ośrodek sprężysto-lepki, podatność na pełzanie, wyrównywanie naprężeń efektywnych

1. Introduction

Long-term geodynamic processes have led to the development of the present-day stress state in the lithosphere, which is described as the primary stress state of the rock mass in mining research. Geomechanical calculations usually assume that the primary stresses resulted from mass forces and, consequently, the absolute values of horizontal stresses are smaller than those of vertical ones [e.g. Sałustowicz 1965]. It is further assumed that Poisson's coefficient is increasing with depth, and the stress differences are reduced (Brown & Hoeck, 1978). *In situ* measurements indicate that the observed distribution of stresses is considerably different from the distribution resulting from the present-day mass loads in certain areas (Amadei & Stephansson, 1997). It was found that, close to the continental plate motion and active orogenesis, horizontal stresses exceed vertical ones even several times at small depths. Such an primary stress state may essentially influence mining conditions and the method of deposit cuper excavation, e.g. in the Polish LGOM Basin (Butra et al., 2011). It is also known that non-homogeneous rock mass considerably influences the distribution of primary stresses; in particular, the rock density and rheological properties differences cause salt-dome uplifting, but with the occurrence of hydrostatic stress state in salt (Ode, 1968). The process of primary stress development on salt rocks can be simulated under model testing (Kortas, 2006).

In the mathematical models used for the determination of stress and strain states around mine workings (Filcek et al., 1994), the primary stress state constitutes the initial condition of the resolution of the systems of partial differential equations. The properties of rocks are usually studied by laboratory methods, with *in situ* examinations applied to the behaviour of the media made up of such rocks. Respective model tests with numerical analysis allow for the search for relationships between physical and time-space variables which reflect the behaviour of the given medium in the assumed mathematical model. An example of that approach consists in the determination of the development of stress in time, depending on the strain properties of particular stress areas, which is the subject-matter of the present research. The recognition of the primary stresses shaping process in that way is important for both knowledge and practice development.

This paper presents model research results concerning the changes of stress in time, in both homogeneous and non-homogeneous rock masses, with the rock mass being represented by a layer with separate strain properties in respect to the surrounding medium.

2. Research Method

Our research on the rock mass behaviour was conducted by representation of the rock mass with elastic-viscous medium with the power creep law, similarly to e.g. (Ślizowski, 2006). When discussing the research method, the following were introduced: (i) description of the physical model, giving constitutive relationships of stress and strain in time, (ii) description of the assumed geometrical model, which represents a simple non-homogeneous form of the medium composed of a layer and its surroundings, and (iii) the properties of a certain hyperbolic function which was later applied to the analysis of the model study results.

2.1. Physical Model

The numerical analysis relied on linear Hooke's law which can be transcribed in the form of two tensor equations (1), binding stress and strain, of which one describes the shape change law and the other one the bulk change law:

$$ {}^{D}\varepsilon_{ij} = \frac{1+\nu}{E}\,{}^{D}\sigma_{ij}\,; \qquad {}^{A}\varepsilon_{m} = \frac{1-2\nu}{E}\,{}^{A}\sigma_{m} \tag{1} $$

Where strain deviator: ${}^{D}\varepsilon_{ij} = \varepsilon_{ij} - {}^{A}\varepsilon_{m}\delta_{ij}$ (δ_{ij} – Kronecker's delta), stress deviator: ${}^{D}\sigma_{ij} = \sigma_{ij} - {}^{A}\sigma_{m}\delta_{ij}$, strain: ${}^{A}\varepsilon_{m} = {}^{1}/_{3}(\varepsilon_{11} + \varepsilon_{22} + \varepsilon_{33})$ and stress: ${}^{A}\sigma_{m} = {}^{1}/_{3}(\sigma_{11} + \sigma_{22} + \sigma_{33})$.

To simulate viscous behaviour, we used the Norton-Bailey power creep law, determined by the dependence of strain rate on the stress state and the time t:

$$ \dot{\varepsilon}_{ij} = \frac{3}{2} mA \exp\left(-\frac{Q}{RT}\right) \sigma_{ef}{}^{n-1} \sigma_{ij} t^{m-1} \tag{2} $$

where Q is the activation energy, R is the gas constant, T is temperature in Kelvin, and A is the material constant. The dependence of strain on the values of n and m in the Norton-Bailey power creep law is discussed in (Maj, 2012); in our calculations, the following assumptions were made: $n = 2$ and $m = 1$. For those constants, equation (2) has the form of $\dot{\varepsilon}_{ij} = {}^{3}/_{2} B \sigma_{ef} \sigma_{ij}$.

The function of the material constants A, Q, and R in (4), in the specific temperature T, defines the material's creep compliance B, determined by equation:

$$ B = A \exp\left(-\frac{Q}{RT}\right) \tag{3} $$

Practically, creep process activation energy Q is not determined for rocks, and R is a universal physical constant equal to the work effected by heating 1 mol of perfect gas by 1 degree Kelvin, being equal to 8.314462 J/(mol*K). For that reason, the determination of the value $B(T)$ is the actual result of laboratory tests.

In the strain process of the medium under a constant load, the effective stress s_{ef}, expressed by principal stresses s_1, s_2, and s_3 in (4), is changing in time:

$$ \sigma_{ef}(t) = \frac{1}{\sqrt{2}} \sqrt{[\sigma_1(t) - \sigma_2(t)]^2 + [\sigma_2(t) - \sigma_3(t)]^2 + [\sigma_3(t) - \sigma_1(t)]^2} \tag{4} $$

The process of stress equilizing and medium strain development, initiated by mass load, occurs only if $\sigma_{ef}(t) > 0$ and $B \neq 0$ in certain medium zones. The process is concluded when the principal stress components are identical, that is $\sigma_{ef} = 0$. Therefore, effective stress may be a quantifier of the stress equilizing process.

In the medium with the power creep law, multiplication, division, involution, or logarithming in constitutive equations correspond to addition, substraction, multiplication, and division in a linear medium, respectively. Therefore, let the value β determine the power change of the value of viscous properties from ${}^{1}B$ to ${}^{2}B$:

$$ \beta = \log({}^{2}B / {}^{1}B) \tag{5} $$

Then, each increase of β by 1.0 corresponds to the ten time increase of the creep compliance B. Similarly, one can define h as a power change of the bulk rigidity modulus. At the specific value of Poisson's coefficient ν, the diversity of the bulk rigidity modulus (Helmholtz modulus) $E/[3(1-2\nu)]$ can be reduced to the function of Young's elongation strain modulus E:

$$\eta = \log({}^{2}E/{}^{1}E) \quad \text{for} \quad \nu = \text{const} \tag{6}$$

In that approach, the values of h and b are the parameters of shear and bulk strain changes in the medium.

2.2. Geometric Model and the Method of Study

The primary geometric stress model adopted for stress equalizes testing was a medium composed of a layer and its surroundings, each with different physical properties. The same rock-mass geometric model, presented in Fig. 1, was adopted for all calculations. In that model, a layer sloping at 20°, with constant vertical thickness of 15 m, was different than its surroundings. The layer's centre was located at the depth of 234 m, within a rectangle of the horizontal dimension of 330 m and the vertical one of 300 m. Within the small rectangle MNOP (Fig. 1), average stress values were calculated. The occurrence of an anhydrite layer on the southern edge of the Fore-Sudeten Monocline can be an example of the corresponding conditions (Kortas & Maj, 2012).

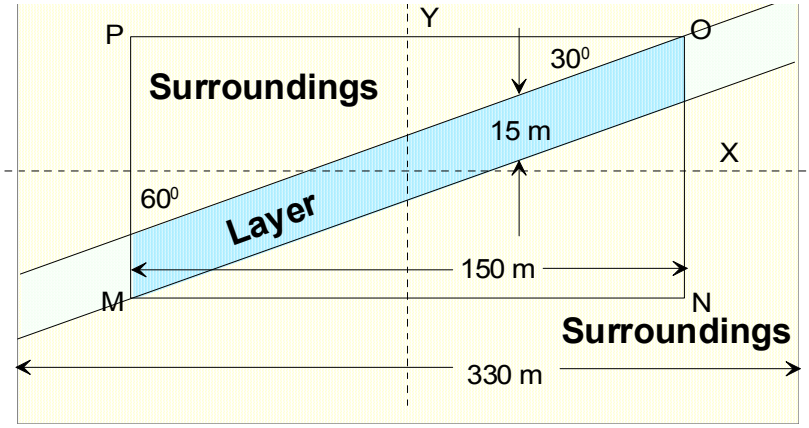

Fig. 1. Geometric Model

Numerical calculations were conducted by the finite element method, with the assumption of the plain state of strain, with the zero displacement boundary condition in horizontal direction. The values of $\sigma_{ef}(t)$, changing in time, were the searched study results, calculated here as the average value of the effective stresses obtained in part of the layer, in the horizontal distance of ±75 m from the centre of the model (Fig. 1).

The sets of tasks, parameterized with the variables, created series of tasks. A graphic presentation of the obtained functional relationships for several series of tasks revealed the relationships between stresses, strain properties, and time that were looked for under model studies.

2.3. The Function of Stress Equilizing in Time

In the rock mass that is susceptible to creep, the initiation of the diversity of effective stresses occurs, resulting from sudden changes in loads caused for example by a tectonic motion, with the drop of effective stresses resulting from long-term rheological processes. The process of changes in stress can be simulated in the first approximation by studying, after applying preliminary load, the behaviour of a model of medium in the time τ. When simulating a lithostatic process in rock salt (e.g. Kortas, 2006), it was found that the stresses existing in a medium that had viscous properties were subjected to equalization or equilizing after the initial elastic reaction ($\tau = 0$) at the time ($\tau \to \infty$):

$$\sigma_{\min}(0) = \sigma_1 < \sigma_2 < \sigma_3 = \sigma_{\max}(0) \to \textit{lithostatic process} \to \sigma_1 = \sigma_2 = \sigma_3 = \sigma_{\max}(\infty).$$

During the simulation of the equilizing of stresses in the time t, we can distinguish three periods: (i) in the first short period (until the time τ_p), the principal stresses are slightly different from the initial stresses resulting from elastic reaction, (ii) the second period ($\tau_p \le \tau \le \tau_k$) is the basic period of stress equilizing, (iii) in the third period ($\tau_k < \tau$), the differences in the principal stress values disappear, and, after a very long time, principal stresses are almost the same.

Let the non-nominal value parameter ζ, with the conventional value belonging to the range of $0 < \zeta < 0.01$ serve the determination of the boundaries of the three periods of principal stress equilizing. Then, through parameter ζ, the times of the beginning τ_p and of the end τ_k of the second stress balance period are correlated with the boundary values of the effective stresses by equation:

$$\zeta \overset{def}{=} \frac{\sigma_{ef}(0) - \sigma_{ef}(\tau_p)}{\sigma_{ef}(0)} = \frac{\sigma_{ef}(\tau_k) - \sigma_{ef}(\infty)}{\sigma_{ef}(0)} \tag{7}$$

That concerns the plain state of strain $\sigma_2(\tau) = \sigma_3(\tau)$. In the homogeneous rock-mass model, the elastic reaction to the mass load p_z causes the development of principal stresses that are directly proportional to the depth H (in the direction Y in Fig. 1) and the density of the medium ρ, that is:

$$\begin{aligned} \sigma_1 &= \sigma_{\min} = H\rho g = p_z \\ \sigma_2 &= \sigma_2 = \sigma_{\max} = p_z[\nu/(1-\nu)] \end{aligned} \tag{8}$$

In the plain state of strain, the effective stress corresponds to the difference between the maximum and minimum principal stresses:

$$\sigma_{ef} = \sigma_{\max} - \sigma_{\min} = \frac{1-2\nu}{1-\nu} p_z \tag{9}$$

During the under discussion process, the stresses $\sigma(\tau)$ change from the initial value of s(0) to the final value of $\sigma_{ef}(\infty) = 0$. Let that change in the medium with a power creep law be described by decreasing hyperbolic function (10), with three constants C_p, C_k, and τ_c, in the form of:

$$\sigma(\tau) = \frac{C_p}{1 + \tau/\tau_c} + C_k \tag{10}$$

If in (10), for the average stresses of $\sigma = \sigma_m$ and the maximum stresses of $\sigma = \sigma_{\max}$, the time $\tau \to \infty$, then $\sigma(\tau) \to \sigma_{\min}$ and $C_k = \sigma_{\min}$. For the effective stresses of $\sigma = \sigma_{ef}$, reducing to zero

with time, the constant $C_k = 0$. At the beginning of the process $\tau = 0$, the stresses: $\sigma = \sigma_m = \sigma_m(0)$, $\sigma = \sigma_{\max} = \sigma_{\max}(0)$ and $\sigma = \sigma_{ef} = \sigma_{ef}(0)$. Let $\sigma(\tau_c) = \sigma(0)/2$ in the time τ_c. Then $\sigma(\tau_c) \approx [C_p - C_k]/2$, and for effective stresses: $\sigma_{ef}(\tau_c) = \sigma_{ef}(0)/2$. Upon introduction of the values of those constants to (10), we can determine the particular functions $\sigma_{\max}(\tau)$, $\sigma_{\min}(\tau)$, and $\sigma_m(\tau)$. Function (10) will have the following form for effective stresses:

$$\sigma_{ef}(\tau) = \frac{\sigma_{ef}(0)}{1 + \tau / \tau_c} \tag{11}$$

Transformations of equations (7) and (11) will produce simple relations (12), binding τ_p, τ_k, and τ_c with ζ:

$$\tau_p = \frac{\zeta \tau_c}{1-\zeta}, \quad \tau_k = \frac{(1-\zeta)\tau_c}{\zeta}, \quad \frac{\tau_p}{\tau_k} = \frac{\zeta^2}{(1-\zeta)^2} \approx \zeta^2, \quad \tau_c = \sqrt{\tau_p \tau_k} \tag{12}$$

With those assumptions, for a small value of ζ, the constant of the stress equilizing process τ_c, called here the period of half-way equilizes of stresses, is the geometric average of the times τ_p and τ_k, determined by functions (7) and (11). Function (11) was applied to the approximation of the results of the model studies concerning the stress state equilizing processes in the layer and its surroundings.

3. Research Results and Result Analysis

The results of the completed model studies are presented in two sections below. In the first case, with the assumption of a homogeneous rock mass, the layer and its surroundings displayed the same geomechanical properties, and in the second case, the properties of the layer and of its surroundings were diverse. The selected values of the shear and bulk strain parameters of the layer and its surroundings, as well as the calculated average values of the effective stresses, were tabularized and presented graphically as a function of time.

3.1. Research Results for a Homogeneous Medium

The purpose of the initial studies was to determine the relationship between the stress equilizing process and the elastic and viscous properties of a homogeneous rock mass. The preliminary series of tasks assumed the following: E = 17 GPa, ν = 0.15, and $B = 5*10^{-28}$ $Pa^{-2}s^{-1}$. Stress equilizing was simulated during the period of $3.16*10^{13}$ s, or 100,000 years. Table 1 contains the values of average principal, effective, and average stresses, calculated in several time periods, and Fig. 2 shows the respective graphs in the time function.

For the time $\tau = 0$, $\sigma_{min} = -5.05$ MPa, $\sigma_{\max} = -0.89$ MPa, and $\sigma_{ef} = 4.16$ MPa were obtained in the central sector of the layer. In the second and basic period of the studied process, the minimum principal stress was constant: $\sigma_{\min}(\tau) = \text{const}$; however, with the increase of time, the maximum principal stresses were dropping: $\sigma_{\max}(\tau) \rightarrow \sigma_{\min}$ and $\sigma_{ef}(\tau) = \sigma_{\max}(\tau) - \sigma_{\min}(\tau) \rightarrow 0$ (Fig. 2). Assuming $\zeta = 0.005$, the boundary values of the effective stresses of the second period of stress equilizing amounted to $\sigma_{ef}(0) - \sigma_{ef}(\tau_p) = 0.025$ MPa, $\sigma_{ef}(\tau_k) - \sigma_{ef}(\infty) = 0.025$ MPa, tending to $\sigma_1(\infty) = \sigma_2(\infty) = \sigma_3(0) = \sigma_{\min}$ after the conclusion of the process.

TABLE 1

Average values of stresses within the layer

τ	$\sigma_1 = \sum_i {}^i\sigma_1$	$\sigma_2 = \sum_i {}^i\sigma_2$	$\sigma_3 = \sum_i {}^i\sigma_3$	$\sigma_{ef} = \sum_i {}^i\sigma_{ef}$	$\sigma_{sr} = \frac{1}{3}\sum_i ({}^i\sigma_1 + {}^i\sigma_2 + {}^i\sigma_3)$
s	MPa	MPa	MPa	MPa	MPa
$3*10^{0}$	–0.884	–0.884	–5.0096	4.1250	–2.2592
$3*10^{-7}$	–0.887	–0.891	–5.0096	4.1229	–2.2610
$3*10^{-10}$	–2.612	–2.612	–5.0096	2.3972	–4.4115
$3*10^{-13}$	–5.006	–5.006	–5.0096	0.0035	–5.0073
$3*10^{-16}$	–5.009	–5.009	–5.0096	0.0004	–5.0095

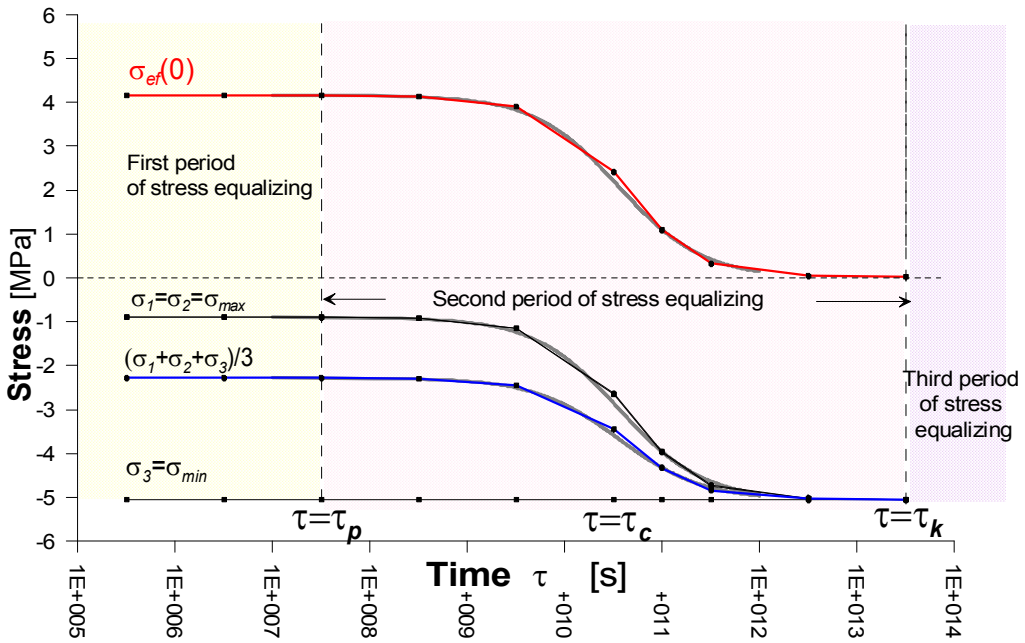

Fig. 2. Average principal and effective stresses in the layer, in the function of time

The examples of the distribution of the average effective stresses at the beginning and at the end of the simulated stress equilizing process are illustrated in Fig. 3.

In the initial series of tasks, the stress equilizing process was simulated with the constants values of the medium's viscous properties and diverse elastic property values. The assumed parameters are presented in Table 2 (series 1-4) and the results in Fig 4.

Function (11) was applied to the approximation of the calculation results presented in Fig. 2, marking with upper index the task series numbers in Table 2.

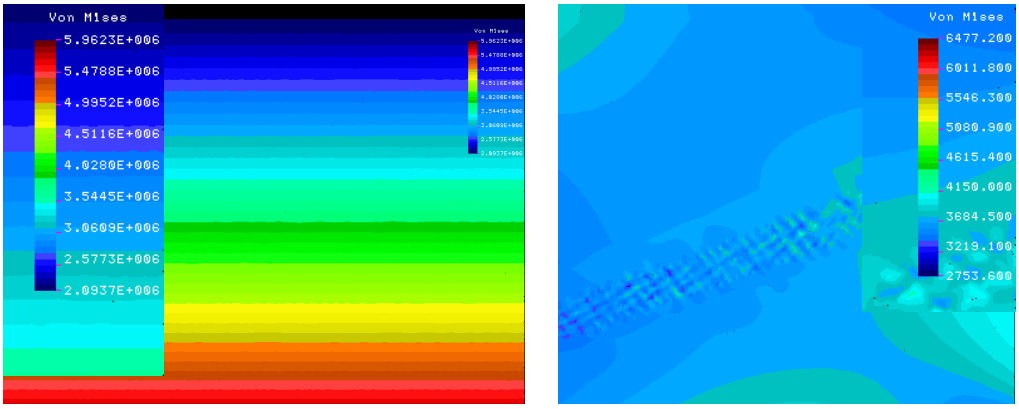

Fig. 3. Distribution of the effective stress $\sigma_{ef}(x, y, \tau)$ [Pa]:
Left: ($\tau = 0$ s) Max(σ_{ef}) = **5.96** MPa; Right: $\tau = 3*10^{13}$ s) Max(σ_{ef}) = **0.004** MPa

TABLE 2

The values of variables and constants of the medium in task series from 1 to 6

Series No.	E [GPa]	ν [1]	B [Pa^{-2}s^{-1}]	τ [s]	$\sigma_{ef}(0)$ [MPa]	B_c [Pa^{-2}s^{-1}]	τ_c [s]
1	17	0.15	$5*10^{-28}$	from $3.15*10^{5}$ to $3.15*10^{13}$	4.16	–	$0.34*10^{12}$
2	1	0.30	$5*10^{-28}$	from $3.15*10^{5}$ to $3.15*10^{14}$	2.89	–	$8.33*10^{12}$
3	17	0.30	$5*10^{-28}$	from $3.15*10^{5}$ to $3.15*10^{13}$	2.89	–	$8.33*10^{12}$
4	1	0.15	$5*10^{-28}$	from $3.15*10^{5}$ to $3.15*10^{14}$	4.16	–	$0.34*10^{12}$
5	1	0.15	$5*10^{-25}$	from $1.00*10^{3}$ to $1.00*10^{11}$	4.16	–	$0.34*10^{9}$
6	1	0.15	$5*10^{-22}$	from $3.15*10^{2}$ to $3.15*10^{6}$	4.16	–	$0.34*10^{6}$
7	1	0.15	from $5*10^{-29}$ to $5*10^{-23}$	$1*10^{5}$ s	4.16	$4*10^{-26}$	–
8	1	0.16	from $5*10^{-29}$ to $5*10^{-18}$	$1*10^{10}$ s	4.15	$4*10^{-21}$	–

The test results indicated that, with the constant creep compliance B, the following were obtained in task series 1 and 4:

- For series 1 and 4 ($\nu = 0.15$), identical values of $\sigma_{ef}(0) = 4.16$ MPa and identical times of half-way effective stress equilizing: ${}^{1}\tau_c = {}^{4}\tau_c = 0.357*10^{10}$s.
- For series 2 and 3 ($\nu = 0.30$), identical values of $\sigma_{ef}(0) = 2.89$ MPa and identical times of half-way effective stress equilizing: ${}^{2}\tau_c = {}^{3}\tau_c = 8.33*10^{11}$ s.
- The change of $\sigma_{ef}(0)$ in series 1 and 3, as well as 2 and 4, resulting from the change of the Poisson coefficient value, in accordance with equation (9).

For the conditions B = const and ν = const, the relationship of the two $\tau_c(E)$ values is approximately inversely proportional to the value E and proportional to $\sigma_{ef}(0)$:

$$\frac{{}^{2}\tau_c({}^{2}E)}{{}^{1}\tau_c({}^{1}E)} \approx \frac{{}^{2}\sigma_{ef}(0)}{\eta\,{}^{1}\sigma_{ef}(0)}, \quad B = \text{const}, \quad \nu = \text{const} \tag{13}$$

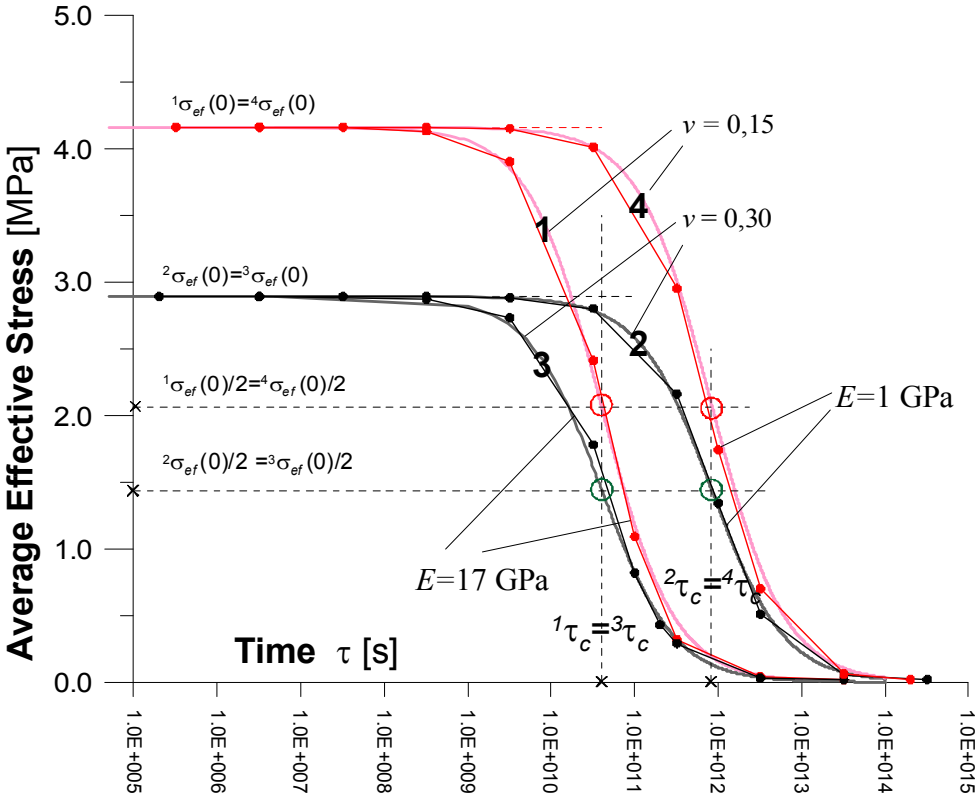

Fig. 4. The dependence of the layer's $\sigma_{ef}(\tau, E, \nu)$ on the stress equalizing time; parameters: E and ν

Therefore, with the drop of the modulus E, the time of half-way stress equilizing is increasing.

Subsequent tests of task series 5 and 6 (Table 2) consisted in checking the influence of the changes in the creep compliance of the medium B on the stress equilizing process. The respective calculations were conducted with the same values of elastic properties. The simulation results are presented in Fig. 5.

The simulations $\sigma_{ef}(\tau, B)$ indicated that, at the specific values of elastic properties, the string of applied values of the parameter B led to the generation of similar graphs (Fig. 5). The value of $\sigma_{ef}(0)$ does not depend on the medium's creep compliance. With the decrease of creep compliance value, the times τ_p, τ_c, and τ_k are increasing. The relationship between creep compliance and the half-way stress equilizing time τ_c is then expressed by this proportion:

$$\frac{^2\tau_c}{^1\tau_c} = \frac{^1B}{^2B}, \text{ or } \frac{^2\tau_c}{^1\tau_c} = 10^{\beta}, \quad E = \text{const}, \quad \nu = \text{const} \tag{14}$$

The influence of the change of the creep compliance $^1B \rightarrow {}^2B$ can be reduced to equation:

$$\sigma_{ef}(^2\tau_c, {}^2B) = \sigma_{ef}(^1\tau_c\, {}^1B/{}^2B, {}^1B) \tag{15}$$

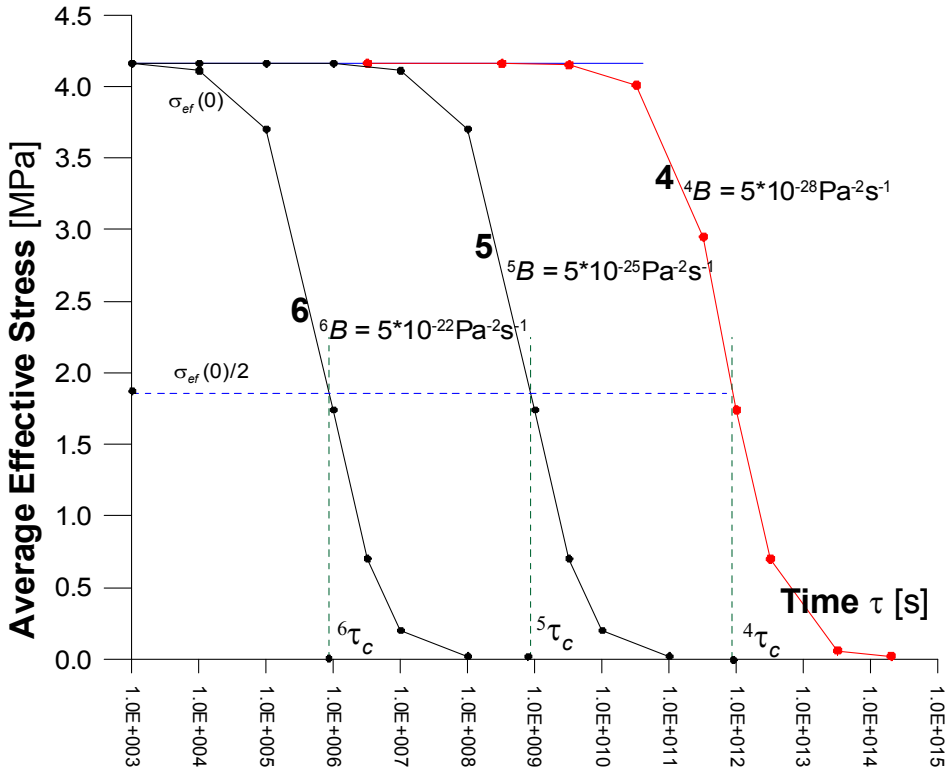

Fig. 5. The dependence of the layer's $\sigma_{ef}(\tau, B)$ on the stress equalizing time; parameter: B

Since for the specific z the time of the conclusion of the second stress equilizing period τ_k is increasing with the value of τ_c (11), together with the decrease of creep compliance; therefore, the lower the rock mass's creep compliance the longer the stress equilizing period. The duration of the second stress equilizing period is then inversely proportional to creep compliance. And thus, for series 6: $\tau_c \approx 10^8$ s and for series 4: $\tau_c \approx 10^{14}$ s (Fig. 5).

Model studies demonstrated that the influence of creep compliance on the stress equilizing is similar as process depends on duration. Consequently, in function (11), instead of the time τ, we can use the variable B, an time will be a process parameter as a constant, that is:

$$\sigma_{ef}(B) = \frac{\sigma_{ef}(0)}{1 + B / B_c}, \quad \text{where } \tau = \text{const}, \quad \sigma_{ef}(0) = \lim_{B \to 0} \sigma_{ef}(B) \tag{16}$$

Consequently, instead of the constant τ_c in (11), there is B_c in (16): the creep compliance at which half-way effective stress equilizing occurs, in the time τ = const adopted in the task series. Irrigation of silt formation, or rock fracturing and crushing, are the examples of the process leading to the increase of the rock's creep compliance.

Similarly to the influence of time on stresses, shown in Fig. 2, we can identify three periods of the influence of creep compliance on effective stress equilizing (Fig. 6). The creep boundaries in

the second period are associated with the small conventional value of ζ, defined as in formula (7), but with τ_p and τ_k replaced by B_p and B_k, respectively.

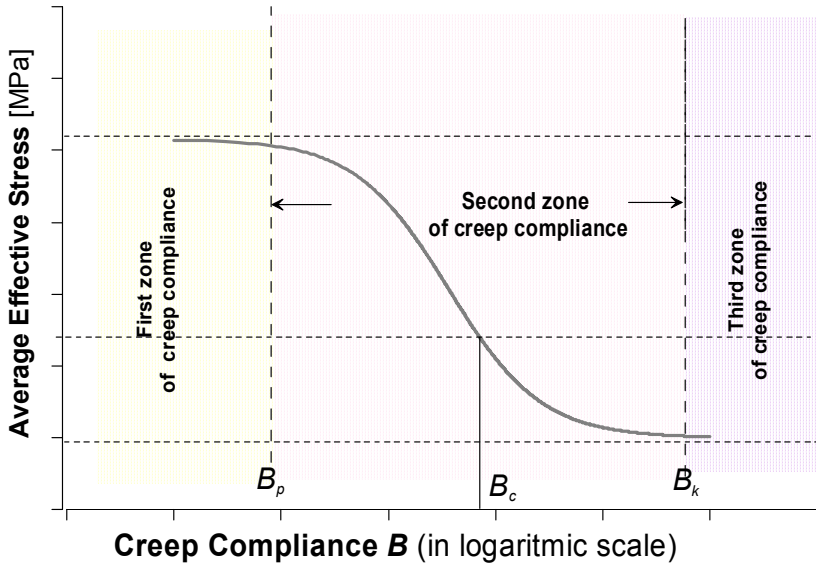

Fig. 6. The zones of the influence of creep compliance on stress equalizing, for the time τ_k = const

In zone (i), $B < B_p$, the creep compliance value does not significantly influence the change of the maximum values of σ_{ef}, in zone (ii), $B_p < B < B_k$, the increase of creep compliance essentially influences stress equilizing, and in zone (iii), $B_k < B$, the increase of the creep compliance value B does not significantly influence the change of the values of σ_{ef} which are close to zero. The value of B_c determines the creep compliance at which half-way effective stress equilizing will occur in the assumed time, or $\sigma_{ef}(B_c) = \sigma_{ef}(0)/2$.

For the specific values of elastic properties, the parameter τ_k is associated with B_c by proportion:

$$\frac{{}^2B_c}{{}^1B_c} = \frac{{}^2\tau}{{}^1\tau} \quad \text{or} \quad \frac{{}^2\tau}{{}^1\tau} = 10^{\beta}, \quad E = \text{const}, \ \nu = \text{const} \tag{17}$$

Fig. 7 presents the results of $\sigma_{ef}(B)$ calculations in two task series, 7 and 8 (Table 2.), for two times: $\tau = \tau_k\, 10^5$ s and 10^{10} s.

According to (17), we received $\log({}^8\tau/{}^7\tau) = \log(10^{10}\text{ s}/10^5\text{ s}) = \log({}^8B_c, {}^7B_c) = \log(4*10^{-21}\text{ Pa}^{-2}\text{s}^{-1}/4*10^{-26}\text{ Pa}^{-2}\text{s}^{-1}) = 5$.

Relationships (18) occur between the creep compliance values of B_p, B_k, and B_c, depending on z, similarly to (12):

$$B_p = \frac{\zeta B_c}{1-\delta}, \quad \tau_k = \frac{(1-\zeta)B_c}{\zeta}, \quad \frac{B_p}{B_k} = \frac{\zeta^2}{(1-\zeta)^2} \approx \zeta^2, \quad B_c = \sqrt{B_p B_k} \tag{18}$$

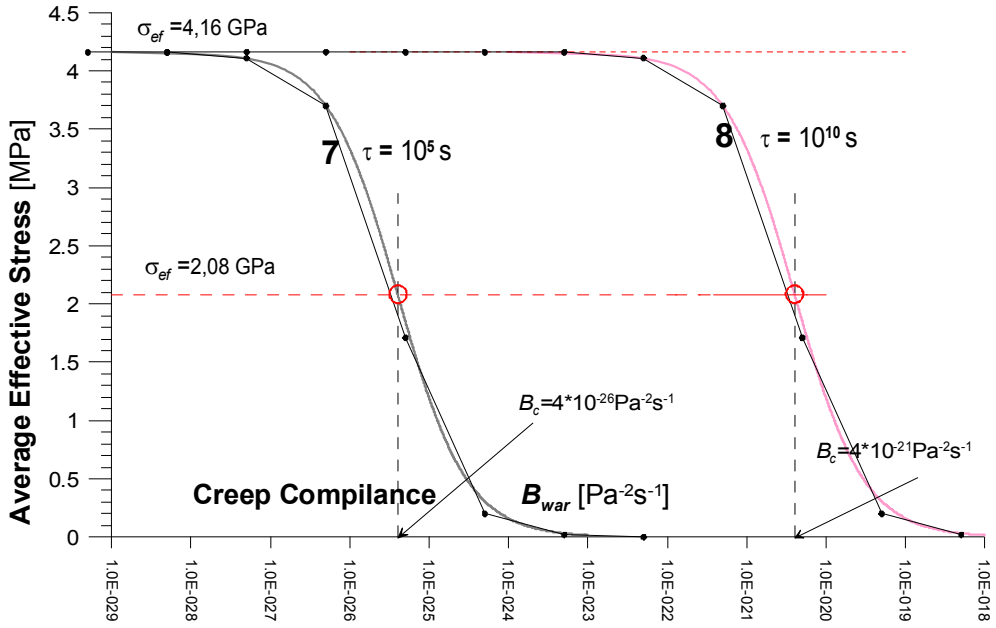

Fig. 7. The dependence of the layer's $\sigma_{ef}(B, \tau)$ on the compliance of the medium B, parameter: τ

Relationships (18) characterized the equilizing of stresses resulting from the increase of creep compliance of the elastic-viscous medium, with power creep law. We should, however, mention that those relationships will be different if a change of bulk strain occurs, together with a change of the medium's creep compliance.

3.2. Research Results for a Non-Homogeneous Medium

The non-homogeneous medium is characterized by diverse properties of its components, i.e. the layer and its surroundings in the model under discussion. Another series of model studies concerned first the influence of the time t on the average effective stresses $\sigma_{ef}(\tau)$ in the layer with the creep compliance of ${}^{war}B = 10^{-28}$ Pa^{-2}s^{-1}, and ${}^{oto}B = 10^{-25}$ Pa^{-2}s^{-1}. In those studies, the creep compliance of the surroundings is higher than that of the layer, while the diversity of the surroundings's creep compliance ${}^{oto}B$ and of the layer ${}^{war}B$ is characterized by $\beta = 3$. Consequently, the layer's creep compliance is by 3 orders lower than that of the surroundings. In the first series of tests (Table 3, series 11-15), the analysts were studying the dependence of effective stresses on time $\sigma_{ef}(\tau, {}^{war}E)$, at specific properties, parameterizing the layer's elasticity modulus ${}^{war}E \in$ [5..100 GPa].

The calculation results are presented in Fig. 8.

Similarly to the homogeneous medium model, the dependence of $\sigma_{ef}(\tau, E)$ is a decreasing function, with asymptote $\sigma_{ef}(\infty, E) = 0$, determining the status after the principal stresses were equalized in the layer. The value of the time τ_c, for which $\sigma_{ef}(\tau_c)$ equals $\sigma_{ef}(0)/2$, is increasing in this series of tasks, with the decrease of the modulus E of the layer. So, for $E = 100$ GPa, $\tau_c \sim 10^9$ s, and for $E = 5$ GPa, $\tau_c \sim 10^{11}$ s (Fig. 8). The increase of the gradient $\Delta\sigma_{ef}(\tau, E)/\Delta E$ before the curve

TABLE 3

Properties, parameters, and variables in the task series concerning the homogeneous medium

Series No.	Variable	Layer			Medium			β
		E	ν	B	E	ν	B	
		MPa	1	$Pa^{-2}s^{-1}$	MPa	1	$Pa^{-2}s^{-1}$	3
11	Time τ	**100**	0.15	$5*10^{-28}$	1.0	0.30	$5*10^{-25}$	3
12		50	0.15	$5*10^{-28}$	1.0	0.30	$5*10^{-25}$	3
13		**25**	0.15	$5*10^{-28}$	1.0	0.30	$5*10^{-25}$	3
14		**17**	0.15	$5*10^{-28}$	1.0	0.30	$5*10^{-25}$	3
15		**5**	0.15	$5*10^{-28}$	1.0	0.30	$5*10^{-25}$	3
16	Time τ	17	0.15	$5*10^{-28}$	1.0	0.30	$\mathbf{5*10^{-25}}$	3
17		17	0.15	$5*10^{-28}$	1.0	0.30	$\mathbf{5*10^{-23}}$	5
18		17	0.15	$5*10^{-28}$	1.0	0.30	$\mathbf{5*10^{-21}}$	7
19		17	0.15	$5*10^{-28}$	1.0	0.30	$\mathbf{5*10^{-19}}$	9
20		17	0.15	$5*10^{-28}$	1.0	0.30	$\mathbf{5*10^{-17}}$	11
21	Time τ	17	0.15	$5*10^{-28}$	1.0	0.30	$\mathbf{5*10^{-23}}$	5
22		17	0.15	$5*10^{-28}$	1.0	0.30	$\mathbf{5*10^{-21}}$	5
23		17	0.15	$5*10^{-28}$	1.0	0.30	$\mathbf{5*10^{-19}}$	5
24	Compliance ${}^{war}B$	17	0.15	$\tau = 3.2^{*}10^{9}$	1.0	0.30	$\mathbf{5*10^{-24}}$	5
25		17	0.15		0.5	0.30	$\mathbf{5*10^{-21}}$	4

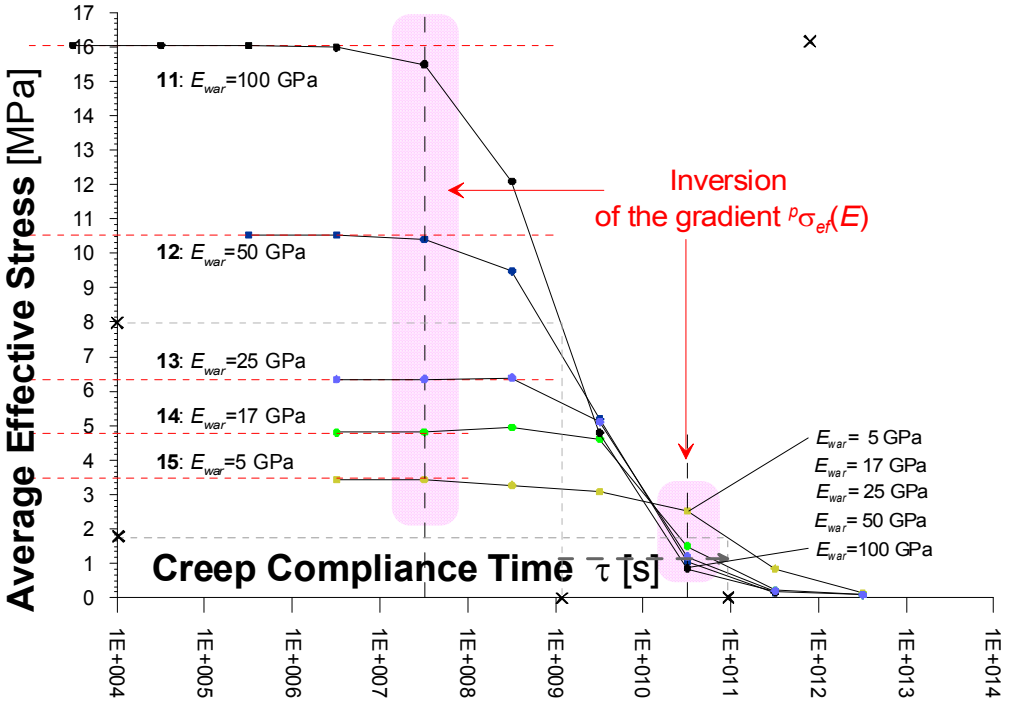

Fig. 8. The dependence of the layer's $\sigma_{ef}(\tau, E)$ at constant time of stress equalizing, parameter: E

bending zone is positive and it is negative afterwards. In the first half of the second period, with the increase of the layer's modulus E (in the range of ${}^{war}E > 5$ GPa) and with the increase ${}^{war}E$, the effective stress is increasing in the layer; however, in the second half, the effective stress is decreasing (Fig. 8). The juxtaposition of effective stresses in the layer's elastic modulus function for $\tau = 0$, corresponding to the immediate reaction and the same for the long-term reaction, is shown in Fig. 9.

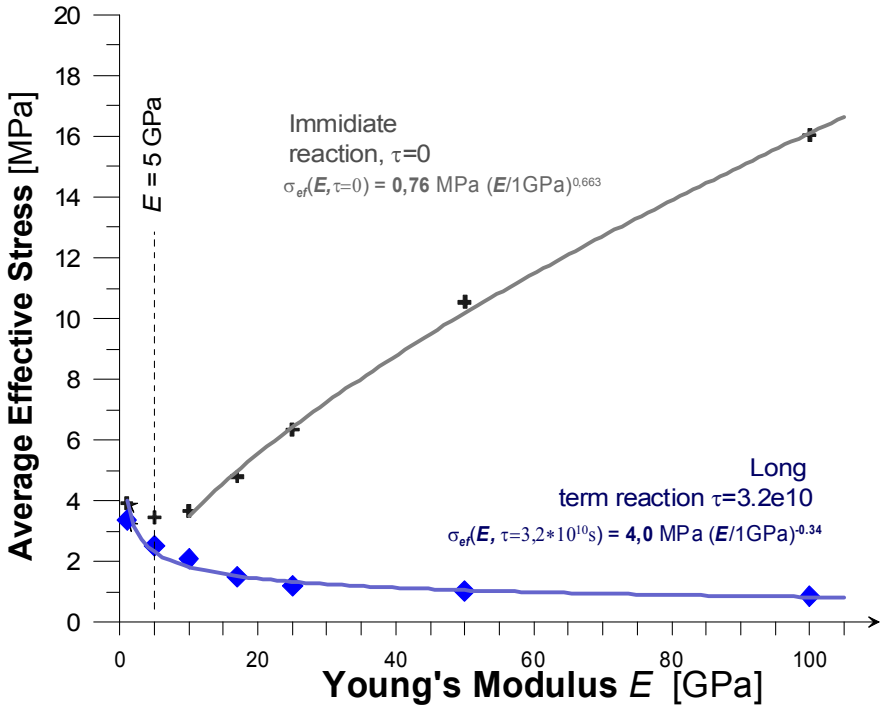

Fig. 9. Inversion of the gradient $\Delta\sigma_{ef}(E,\tau)/\Delta E$ in the time $\tau \in [0..3.2*10^{10}]$

Within the range of the specific values of the layer's elastic modulus $E < 17$ GPa, a local minimum of the function $\mathrm{Min}[\sigma_{ef}(\tau, E)] = 2.2$ MPa is developing. Within the range of $E > 17$ GPa, the immediate reaction corresponding to $\tau \sim 0$, $\sigma_{ef}(\tau, E)$ is the increasing function ${}^{war}E$, which is approximated by the increasing power function with the positive exponent of +0.663 (Fig. 9). However, the long-term reaction, after expiration of a long period of time, is approximated by a decreasing power function, with a negative exponent of –0.34.

Our simulations indicated that, at the values of ${}^{war}E \in [17..25$ GPa], within the range of $\tau \in [10^8..10^9$s], there occurs a local extreme value for the time $\tau_e = 3.16^*10^8$.

Subsequent calculations (Table 3, task series 16-20) were concentrating on the determination of the influence of the surroundings's creep compliance ${}^{oto}B$ on the position of the extreme value of $\sigma_{ef}(\tau_e) = \mathrm{Max}[\sigma_{ef}(\tau)]$, or the determination of the time τ_e. In this task series, constant values of the elastic properties and the constant value of the layer's creep compliance ${}^{war}B = 5*10^{-24}$ $\mathrm{Pa}^{-2}\mathrm{s}^{-1}$ were preserved, with the change of the surroundings's creep compliance. It was found that

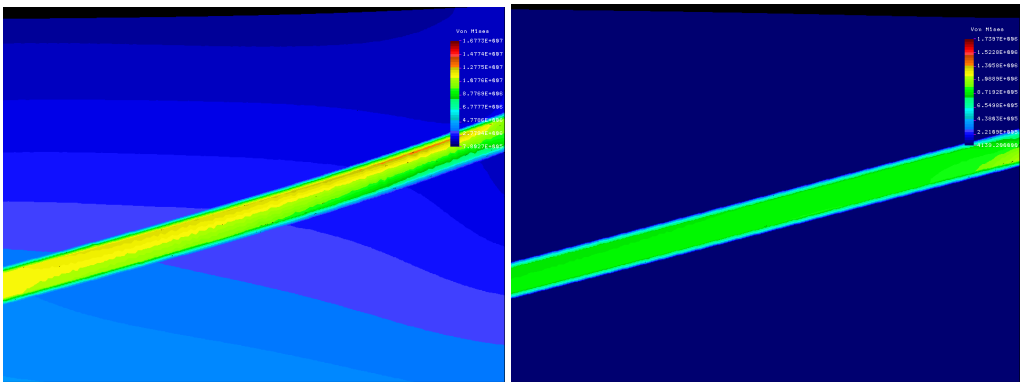

Fig. 10. The distribution of effective stresses $\sigma_{ef}(x, y, \tau)$ [Pa]. Left: $E = 50$ GPa and $\tau = 3.16*10^{9}$, Max(σ_{ef} = 17.8 MPa); Right: $E = 5$ GPa and $\tau = 3.16*10^{12}$, Max(σ_{ef} =1.7 MPa)

with the increase of $\beta = \log({}^{oto}B/{}^{war}B)$, within the range of $\beta \geq 5$, the values of $\sigma_{ef}(0) = 4.79$ MPa and $\sigma_{ef}(\tau_e)$ = Max $\sigma_{ef}(\tau) = 5.37$ MPa did not change, although the value of τ_e was changing in a specific manner (Fig. 11). Within the range of $\beta < 5$, together with the decrease of b down to 0, the effect of the extreme value occurrence is decreasing and it disappears at $\beta = 0$, corresponding to medium's homogeneous model conditions.

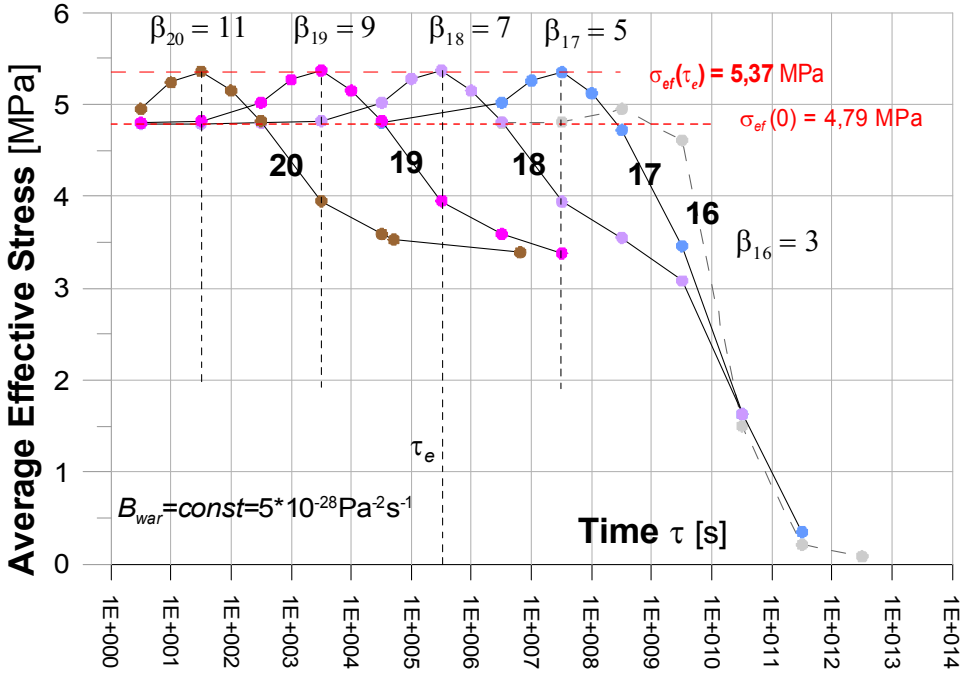

Fig. 11. The dependence of $\sigma_{ef}(\tau, \beta)$ on the stress equalizing time; parameter: β, with the indicator corresponding to the series number of Table 3

With the preservation of the specific value β in the cycle of simulation, a similar effect is caused by the change of the creep compliance of the layer and its surroundings. Fig. 12 presents three curves whose parameters fulfill the condition $\beta = 5$. It was found that the increase of the surroundings's creep compliance value ${}^{2oto}B > {}^{1oto}B$ led to the decrease of τ_e by the number of orders equal to the number of the orders of creep compliance's increase, without a change of the maximum value of $\sigma_{ef}(\tau_e)$. So, for example, in two series of tasks for ${}^{war}B$ = const and ${}^{oto}B$, the increase was by 2 orders higher: $3*10^{-23}$ Pa^{2}s^{-1} to $3*10^{-21}$ Pa^{2}s^{-1}. However, for ${}^{oto}B$ = const, the layer's creep compliance ${}^{war}B$ decreased from $3*10^{-28}$ Pa^{2}s^{-1} to $5*10^{-30}$ Pa^{2}s^{-1} causing reduction of the time τ_e from $5*10^7$ s to $5*10^5$ s.

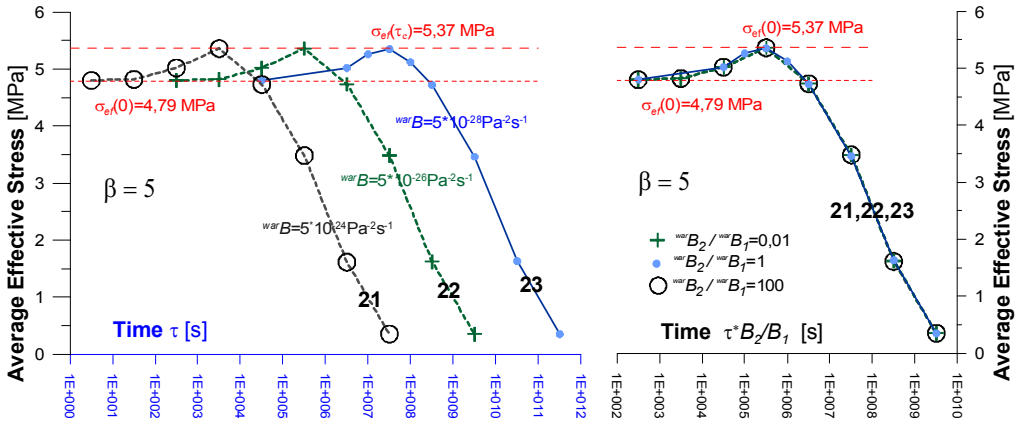

Fig. 12. The dependence of $\sigma_{ef}(\tau, {}^{war}B)$ on the stress equalizing time; parameter: creep compliance ${}^{war}B$, with the condition $\beta = 5$

The graphs of those curves are parallel in the logarithmic scale of time (Fig. 12); therefore, the shift of a curve owing to the change of the layer's creep compliance from ${}^{war}B_1$ to ${}^{war}B_2$ is directly proportional to the quotient of ${}^{war}B_2 / {}^{war}B_1$, and it is expressed by the following function in case of the constant value of the proportion ${}^{oto}B / {}^{war}B$:

$$\sigma_{ef}({}^{war}B_1, \tau) \approx {}^{p}\sigma_{ef}({}^{war}B_2, \tau {}^{war}B_2 / {}^{war}B_1), \quad \text{for } \beta = \log({}^{oto}B / {}^{war}B) = \text{const} \tag{19}$$

That relationship expresses the principle that the time of principal stress equilizing in the layer surrounded by the rocks that are more susceptible to creep is directly proportional to the creep compliance of that layer and inversely proportional to the surroundings's creep compliance.

For the conditions of task series 21 (Table 3), we studied the influence of the depth on stress equilizing. With the increase of depth, the initial effective stress was increasing, together with the value of the difference of Max$[\sigma_{ef}(\tau)] - \sigma_{ef}(0)$. After $5*10^{12}$ s, regardless of the assumed depths H, effective stresses were the same (Fig. 13) and close to zero. Therefore, the influence of depth on the stress equilizing process disappeared after a long period.

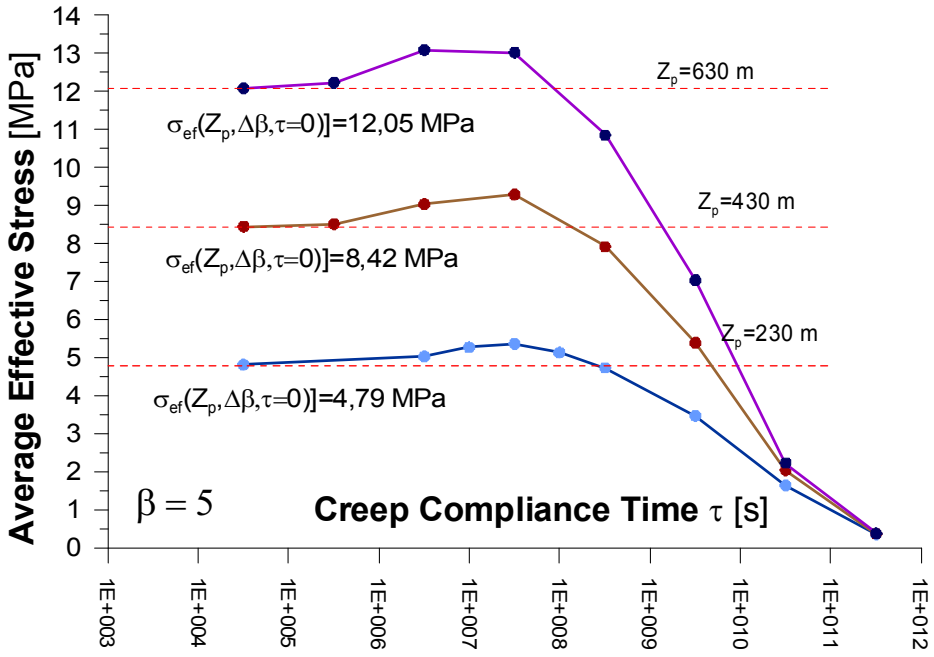

Fig. 13. The influence of depth on effective stresses (for the conditions of series 21, Table 3)

Similarly to the homogeneous medium, effective stresses can be presented as a function of creep compliance and parameterize it with time, using function (16) for approximation. Fig. 14 presents the results of the related calculation for the time $3.16*10^9$ s in two task series 24 and 25, with the specific values of elastic properties (Table 3). In those simulations, creep compliance was a parameter, ${}^{oto}B \in [5*10^{-24}, 5*10^{-21}\ \mathrm{Pa^2 s^{-1}}]$ was the constant, and the layer's creep compliance was the variable. The relationships $\sigma_{ef}(t)$ (Figs. 4 and 7) and $\sigma_{ef}({}^{war}B)$ are similar (Fig. 14).

The initial effective stress is getting close to $\sigma_{ef}({}^{war}B = 0) = 4.82$ MPa, with the decrease of ${}^{war}B \rightarrow 0$ for the conditions of series 24, and in the case of series 25, it is getting close to $\sigma_{ef}({}^{war}B = 0) = 3.39$ MPa. Therefore, the surroundings's creep compliance ${}^{oto}B$ influences the initial value of the layer's effective stress, and the value of $\sigma_{ef}({}^{war}B = 0)$ is increasing with the increase of ${}^{oto}B$. The approximation of the results indicated compliance with function (16); however, only in the range of the values $B < B_c$ (Fig. 14).

4. Summary and Conclusions

Our model studies present the development of the stresses in time, in a layer with a small slope, which layer and their surroundings displays elastic-viscous properties that were simulated by the behaviour of the elastic-viscous medium with the power creep law. Our studies simulated, in a simplified manner, the stress equilizing process in the rock mass and the primary stress state in the rock mass, depending on the rock properties and time. We should mention that the results of our studies refer to the conditions that correspond to our model assumptions.

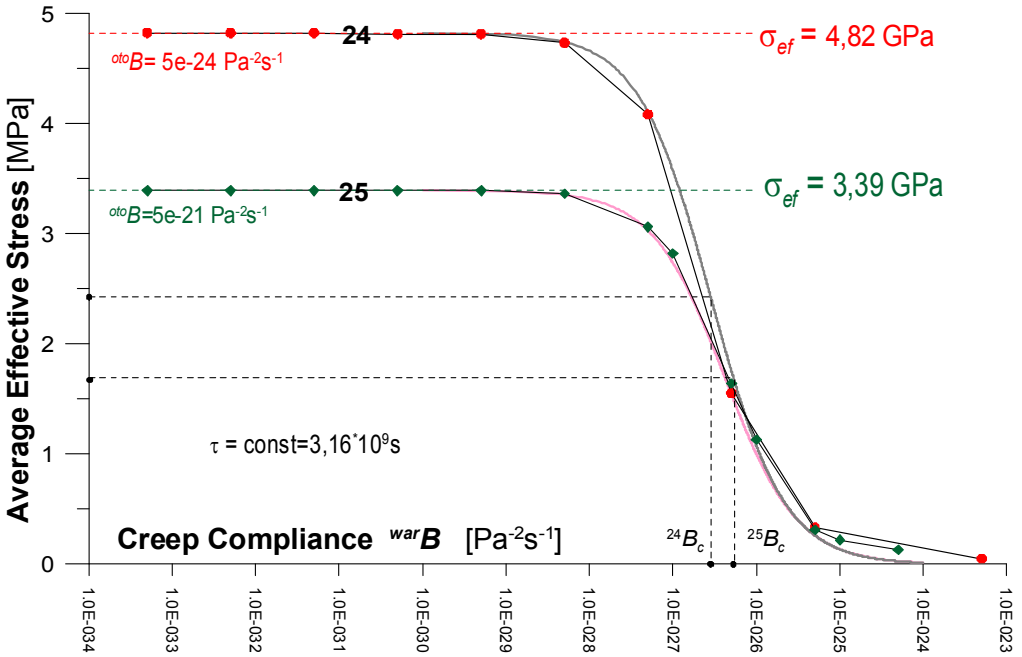

Fig. 14. The dependence of σ_{ef} (^{war}B, ^{oto}B) on the layer's creep compliance at $\tau = 3.16^{*}10^{9}$ = const; parameter: the medium's creep compliance ^{oto}B

In our model studies, we were looking for the stress changes in the layer, as a function of bulk and shear strain of the layer and its surroundings, in which the principal stress differences are decreasing and reducing to zero with time. It was assumed that effective stress was the measure of stress equilizing. Our model studies were conducted for homogeneous and non-homogeneous conditions of the medium.

The following were found in the homogeneous model of the rock mass with uniform properties of the layer and its surroundings:

- The stress equilizing process is well described by hyperbolic function (11) which expresses the principle that the relative increase of stresses is inversely proportional to the measurement variable, which can be either time or creep compliance. The initial value of effective stress for $\tau \sim 0$ or $B \sim 0$ is proportional to the depth and it depends on the value of the Poisson coefficient.
- In the logarithmic scale of time or creep compliance, we can distinguish three periods and ranges. In the second period (Fig. 2) and the second range of changes in creep compliance (Fig. 6), intense effective stress equilizing occurs. For the value of the geometric average of times, at the end of that range τ_c or of the creep compliance B_c, effective stress corresponds to a half of the effective stress recorded at the beginning of the process.
- The increase of the Poisson coefficient does not influence the value of τ_c; however, the increase of Young's modulus of the medium causes the decrease of the value of τ_c. The increase of creep compliance does not influence the initial effective stresses, but it causes the increase of τ_c and of the stress equilizing period.

- The proportions of τ_c of two media that are different in respect of creep compliance correspond to the proportions of their creep compliance rates, and the proportions of B_c of two processes in which creep compliance is the variable correspond to the proportions of respective durations.

The following were found in the non-homogeneous model of the rock mass, with diverse properties of the layer and the surroundings:

- The stress equilizing process only initially complies with hyperbolic function (11). Similarly to the homogeneous medium, the layer's effective stresses are decreasing to zero with time. The initial effective stress is increasing with the increase of the layer's elasticity modulus, and the second stress equilizing period becomes extended. The lower the value of the elasticity modulus, or the lower the differences between the layer's bulk mudulus, the longer is the stress equilizing process.
- With the changes in the creep compliance of the layer and its surroundings, the stress equilizing function is increasing in time and obtains its extreme value. The time at which the said extreme value appears depends on the proportion of the layer's creep compliance to the surroundings's creep compliance. Change in the layer's creep compliance at constant surroundings creep compliance leads to a parallel shift of the effective stress function in the logarithmic scale of time by which the stress equilizing process becomes extended.
- The values of effective stresses with a local extreme value, occurring after a short period, are increasing almost proportionally with depth. After a very long time, the influence of depth disappears.
- Similarly to the homogeneous rock mass, the stress equilizing process can be presented for a variable creep compliance of the layer and time as the parameter, keeping the surroundings creep compliance as a constant.

This study is intended to mention only the relationships of the stress equilizing process with the elastic-viscous medium and time. Particular conclusions concern only the conditions specified in this study. A wider use of those conclusions, especially for the purpose of stress state modelling in the mine working surroundings, would require proper examination of the particular rock-mass properties. However, we can say that, despite such reservations, the results of our studies demonstrate an essential role of time and strain properties in the stress development process in an elastic-viscous medium. The results also indicate that the construction of a geometric rock-mass model, with rheological properties and workings, especially in the case of non-homogeneous media, should be preceded by a calculation analysis, leading to the stress equilizing state, by simulation of the primary lithostatic stress state in the rock mass in that way. Later that stress state will be affected by mine workings.

I wish to thank Dr. Danuta Flisiak for her kind assistance in proof reading.

Reference

Amadei B., Stephansson O., 1997. *Rock stress and its measurement*. Chapman & Hall, Londyn-Weinheim-Nowy Jork--Tokio-Melbourne-Madras.

Brown E.T., Hoek E., 1978. *Trends in relationships between measured rock in situ stresses and depth*. Int. J. Rock Mech. Min. Sci. & Geomech. Abstr. 15, p. 211-215.

Butra J., Dębkowski R., Pawelus D., Szpak M., 2011. *Wpływ naprężeń pierwotnych na stateczność wyrobisk górniczych*. Cuprum, 58 (1).

Filcek H., Walaszczyk J., Tajduś A., 1994. *Metody komputerowe w geomechanice górniczej*. Śląskie Wydawnictwo Techniczne, Katowice.

Kortas G. (red.), 2008. *Ruch górotworu w rejonie wysadów solnych*. Wydawnictwo Inst. Gosp. Surowcami Mineralnymi i Energią PAN, Kraków.

Kortas G., 2006. *Distributions of Convergence in a Modular Structure Projecting a Multi-Level Salt Mine*. Archives of Mining Sciences, Vol. 51, Iss. 4.

Kortas G., Maj A., 2012. *Ekspertyza geotechniczna dotycząca grubości półek stropowych, spągowych oraz filarów dla eksploatacji górniczej złoża „Nowy Ląd" pomiędzy poziomami +35 a -30 m npm*. GeoConsulting dla Kopalni Gipsu i Anhydrytu „Nowy Ląd" w Niwnicach, Kraków, grudzień 2012 (praca niepublikowana).

Kortas G., 2006. *Distributions of Convergence in a Modular Structure Projecting a Multi-Level Salt Mine*. Archives of Mining Sciences, Vol. 51, Iss. 4, p. 547-562.

Maj A., 2012. *Convergence of gallery workings in underground salt mines*. Archives of Mining Sciences, Monograph, No. 14.

Ode H., 1968. *Review of Mechanical Properties of Salt Relating to Salt-Dome Genesis*. Salin Deposits, Geological Society of America, Special Paper 88, s. 543-593.

Sałustowicz A., 1965. *Zarys mechaniki górotworu*. Wyd. Śląsk, Katowice, s. 19-22.

Ślizowski J., 2006. *Geomechaniczne podstawy projektowania komór magazynowych gazu ziemnego w złożach soli kamiennej*. Studia. Rozprawy. Monografie Nr 137, Wyd. IGSMiE PAN, Kraków.